

Aerodynamic roughness parameters in cities: inclusion of vegetation

Article

Published Version

Creative Commons: Attribution 4.0 (CC-BY)

Open access

Kent, C. W., Grimmond, S. ORCID: <https://orcid.org/0000-0002-3166-9415> and Gatey, D. (2017) Aerodynamic roughness parameters in cities: inclusion of vegetation. *Journal of Wind Engineering and Industrial Aerodynamics*, 169. pp. 168-176. ISSN 01676105 doi: <https://doi.org/10.1016/j.jweia.2017.07.016> Available at <https://centaur.reading.ac.uk/71867/>

It is advisable to refer to the publisher's version if you intend to cite from the work. See [Guidance on citing](#).

Published version at: <http://dx.doi.org/10.1016/j.jweia.2017.07.016>

To link to this article DOI: <http://dx.doi.org/10.1016/j.jweia.2017.07.016>

Publisher: Elsevier

All outputs in CentAUR are protected by Intellectual Property Rights law, including copyright law. Copyright and IPR is retained by the creators or other copyright holders. Terms and conditions for use of this material are defined in the [End User Agreement](#).

www.reading.ac.uk/centaur

CentAUR

Central Archive at the University of Reading

Reading's research outputs online



Aerodynamic roughness parameters in cities: Inclusion of vegetation



Christoph W. Kent^{a,*}, Sue Grimmond^a, David Gatey^b

^a Department of Meteorology, University of Reading, Reading, United Kingdom

^b Risk Management Solutions, London, United Kingdom

ARTICLE INFO

Keywords:

Aerodynamic roughness length
Drag coefficient for vegetation
Logarithmic wind profile
Morphometric method
Urban
Zero-plane displacement

ABSTRACT

A widely used morphometric method (Macdonald et al. 1998) to calculate the zero-plane displacement (z_d) and aerodynamic roughness length (z_0) for momentum is further developed to include vegetation. The adaptation also applies to the Kanda et al. (2013) morphometric method which considers roughness-element height variability. Roughness-element heights (mean, maximum and standard deviation) of both buildings and vegetation are combined with a porosity corrected plan area and drag formulation. The method captures the influence of vegetation (in addition to buildings), with the magnitude of the effect depending upon whether buildings or vegetation are dominant and the porosity of vegetation (e.g. leaf-on or leaf-off state). Application to five urban areas demonstrates that where vegetation is taller and has larger surface cover, its inclusion in the morphometric methods can be more important than the morphometric method used. Implications for modelling the logarithmic wind profile (to 100 m) are demonstrated. Where vegetation is taller and occupies a greater amount of space, wind speeds may be slowed by up to a factor of three.

1. Introduction

During neutral atmospheric stratification, the mean wind speed (\bar{U}_z) at a height z , above a surface can be estimated using the logarithmic wind law (Tennekes, 1973):

$$\bar{U}_z = \frac{u_*}{\kappa} \ln \left(\frac{z - z_d}{z_0} \right) \quad (1)$$

where u_* is the friction velocity, $\kappa \sim 0.40$ (Högström, 1996) is von Karman's constant, z_0 is the aerodynamic roughness length, and z_d is the zero-plane displacement. The aerodynamic roughness parameters (z_d and z_0) can be related to surface geometry using morphometric methods (e.g. Grimmond and Oke, 1999; Kent et al., 2017a).

Uncertainties in wind-speed estimations arise from using idealised wind-speed profile relations, as well as representing the surface using only two roughness parameters (z_d and z_0), which are based upon a simplification of surface geometry. Both observations and physical experiments are therefore critical to assess the most appropriate methods to determine roughness parameters and for wind-speed estimation (e.g. Cheng et al., 2007; Tieleman 2008; Drew et al., 2013). Using the logarithmic wind law (Eq. (1)), Kent et al. (2017a) demonstrate that wind speeds estimated up to 200 m above the canopy in central London (UK

most resemble observations using morphometric methods which account for roughness-element height variability (specifically, the Millward-Hopkins et al., 2011 and Kanda et al., 2013 methods). However, an uncertainty of $>2.5 \text{ m s}^{-1}$ exists ($>25\%$ of the mean wind speed) due to the flow variability throughout the profile (Kent et al., 2017a; their Fig. 7).

Bluff bodies (e.g. buildings) and porous roughness elements (e.g. vegetation) have different influences upon wind flow (Taylor, 1988; Finnigan, 2000; Guan et al., 2000, 2003) which need to be accounted for. Although morphometric methods have been developed for only buildings (examples in Mohammad et al., 2015) or vegetated canopies (e.g. Nakai et al., 2008), existing morphometric methods do not consider both solid and porous bodies (i.e. vegetation) in combination.

With the intention of collectively considering buildings and vegetation to determine z_d and z_0 , this work develops the widely-used Macdonald et al. (1998, hereafter *Mac*) morphometric method to include vegetation. The development applies to the more recently proposed Kanda et al. (2013, hereafter *Kan*) development of *Mac* which considers roughness-element height variability. The implications for estimating the logarithmic wind-speed profile (Eq. (1)) up to 100 m above five different urban surfaces are discussed.

* Corresponding author. Room 2U08, Department of Meteorology, University of Reading, Earley Gate, PO Box 243, Reading, RG6 6BB, United Kingdom.

E-mail addresses: C.W.Kent@pgr.reading.ac.uk, c.s.grimmond@reading.ac.uk (C.W. Kent).

Notation	
A_f^*	Unsheltered frontal area of roughness elements
$a_0, b_0, c_0, a_1, b_1, c_1$	Kanda et al. (2013) method constants
A_f	Frontal area of roughness elements
A_p	Plan area of roughness elements
A_T	Total surface area
C_D	Drag coefficient
F_D	Total drag of roughness elements
H_{av}	Average roughness-element height
H_{max}	Maximum roughness-element height
κ	von Karman's constant = 0.4 (Högström, 1996)
L	Obukhov length = $\frac{T u_*^3}{\rho g w T}$
P_{2D}	Two-dimensional porosity
P_{3D}	Three-dimensional or aerodynamic porosity
P_v	ratio of C_{Dv} to C_{Db}
u_*	Friction velocity = $(\overline{(-u'w')^2} + \overline{(-v'w')^2})^{0.25} = \sqrt{\tau/\rho}$
U_z	Wind speed at height z
z_0	Aerodynamic roughness length
z_d	Zero-plane displacement
α	z_d correction coefficient (Macdonald et al., 1998)
β	Drag correction coefficient (Macdonald et al., 1998)
λ_f	Frontal area index of roughness elements
λ_{f-crit}	Frontal area index for peak z_0
λ_p	Plan area index of roughness elements
ρ	Density of air
σ_H	Standard deviation of roughness-element heights
σ_v	Standard deviation of lateral wind velocity (crosswind)
τ	Surface shear stress
Abbreviations	
CC_hv	City centre with high vegetation
CC_lv	City centre with low vegetation
Kan	Kanda et al. (2013) morphometric method
Mac	Macdonald et al. (1998) morphometric method
Pa	Urban park
SB_hv	Suburban area with high vegetation
SB_lv	Suburban area with low vegetation
Additional subscripts	
b	Buildings
v	Vegetation
$l-on$	Leaf-on
$l-off$	Leaf-off

2. Methodology

2.1. Macdonald et al. and Kanda et al. Morphometric methods

Morphometric methods traditionally characterise roughness elements by their average height (H_{av}), plan area index (λ_p) and frontal area index (λ_f). The λ_p is the ratio of the horizontal area occupied by roughness elements ('roof' or vegetative canopy, A_p) to total area under consideration (A_T), whereas λ_f is the area of windward vertical faces of the roughness elements (A_f) to A_T . By including the standard deviation (σ_H) and maximum (H_{max}) roughness-element heights, newer methods consider height variability (Millward-Hopkins et al., 2011; Kanda et al., 2013).

The Mac method is derived from fundamental principles and without assumptions about wake effects and recirculation zones of solid roughness elements (Macdonald et al., 1998), which vary for porous elements (Wolfe and Nickling, 1993; Judd et al., 1996; Sutton and McKenna Neuman, 2008; Suter-Burri et al., 2013). The formulation of z_d and z_0 is (Macdonald et al., 1998):

$$Mac_{z_d} = [1 + \alpha^{-\lambda_p} (\lambda_p - 1)] H_{av} \quad (2)$$

$$Mac_{z_0} = \left(\left(1 - \frac{z_d}{H_{av}} \right) \exp \left[- \left\{ 0.5 \beta \frac{C_{Db}}{\kappa^2} \left(1 - \frac{z_d}{H_{av}} \right) \lambda_f \right\}^{-0.5} \right] \right) H_{av} \quad (3)$$

where the constant, α , is used to control the increase in z_d with λ_p , a drag correction coefficient, β , is used to determine z_0 and C_{Db} is the drag coefficient for buildings. Coefficients can be fitted to observations. For example, using Hall et al.'s (1996) wind tunnel data, Macdonald et al. (1998) recommend $C_{Db} = 1.2$ and $\alpha = 4.43$, $\beta = 1.0$ for staggered arrays; and $\alpha = 3.59$, $\beta = 0.55$ for square arrays. The staggered array values and $C_{Db} = 1.2$ are used here.

Using large eddy simulations for real urban districts of Japan, Kanda et al. (2013) argue that the upper limit of z_d is H_{max} and therefore:

$$Kan_{z_d} = [c_0 X^2 + (a_0 \lambda_p^{b_0} - c_0) X] H_{max}, \quad (4)$$

$$X = \frac{\sigma_H + H_{av}}{H_{max}}$$

and

$$Kan_{z_0} = (b_1 Y^2 + c_1 Y + a_1) Mac_{z_0},$$

$$Y = \frac{\lambda_p \sigma_H}{H_{av}} \quad (5)$$

where $0 \leq X \leq 1$, $0 \leq Y$ and a_0, b_0, c_0, a_1, b_1 and c_1 are regressed constants with values: 1.29, 0.36, -0.17, 0.71, 20.21 and -0.77, respectively.

2.2. Considering vegetation

Although, consideration has been given to treatment of vegetation within building-based morphometric methods (e.g. a reduction of height, Holland et al., 2008), the flexibility, structure and porosity of vegetation suggest the effects upon wind flow and aerodynamic roughness are more complex (Finnigan, 2000; Nakai et al., 2008). During the method development proposed here, vegetation porosity is used, as it is the most common descriptor of the internal structure (Heisler and Dewalle, 1988) and relatively easy to determine (Guan et al., 2002; Crow et al., 2007; Yang et al., 2017). Unlike other characteristics (e.g. structure or flexibility), porosity can be generalised across vegetation types or species with values between 0 (completely impermeable) and 1 (completely porous). Optical (P_{2D}) and volumetric/aerodynamic (P_{3D}) porosity can be related to each other: $P_{3D} = P_{2D}^{0.40}$ (Guan et al., 2003), $P_{3D} = P_{2D}^{0.36}$ (Grant and Nickling, 1998).

The drag of vegetation is also considered, which through absorbing momentum from the wind (Finnigan, 2000; Guan et al., 2003; Krayenhoff et al., 2015) can significantly reduce the surface shear stress (τ) (Wolfe and Nickling, 1993), as well as reduce the exchange between in-canopy and above-canopy flow (Gromke and Ruck, 2009; Vos et al., 2013). The drag generated by vegetation (Wyatt and Nickling, 1997; Grant and Nickling, 1998; Gillies et al., 2000, 2002; Guan et al., 2003) and other porous structures (Seginer, 1975; Jacobs, 1985; Taylor, 1988) varies from that of a solid structure with similar geometry. This variation is more complex than can be resolved by a simple reduction of the frontal area (e.g. Taylor, 1988; Guan et al., 2003). Therefore, the changes in drag are directly considered using the drag coefficient.

Typically, morphometric methods use a single drag coefficient for buildings (C_{Db}), whereas here the drag coefficient of vegetation (C_{Dv}) is also used. The nature and type of vegetation (e.g. size, structure,

flexibility, leaf type) affect C_{Dv} (Rudnicki et al., 2004). In addition, sheltering and the reconfiguration of shape and leaf orientation under varying flow characteristics means a single value for C_{Dv} may be inappropriate (e.g. Guan et al., 2000, Guan et al., 2003; Vollsinger et al., 2005; Pan et al., 2014). Although attempts have been made to separate the form and viscous components of vegetation drag (e.g. Shaw and Patton, 2003), the components tend to be considered in combination (C_{Dv}), as is done here.

The C_{Dv} of foliage typically varies between 0.1 and 0.3 (Katul et al., 2004). From large eddy simulations, Shaw and Schumann (1992) and Su et al. (1998) propose $C_{Dv} = 0.15$. Other numerical simulations suggest $C_{Dv} = 0.25$ (da Costa et al., 2006) and $C_{Dv} = 0.2$ (Zeng and Takahashi, 2000) for pine forests. Field studies in boreal canopies (pine, aspen and spruce) indicate C_{Dv} varies between 0.1 and 0.3 (Amiro, 1990). A C_{Dv} of 0.2 is commonly used in numerical studies of wind flow in vegetated canopies (Van Rennerghem and Botteldooren, 2008). Whereas, rough- and smooth-surface cylinders have $C_D = 1.2$ (Simiu and Scanlan, 1996) or $C_D = 0.8$ (Guan et al., 2000), respectively.

There is evidence that that C_{Dv} varies with wind speed, with higher C_{Dv} at lower wind speeds. Results from wind tunnel studies include: for seven 5.8–8.5 m British forest saplings C_{Dv} varied from 0.88 to 0.15 when wind speeds were between 9 and 26 m s⁻¹ (Mayhead, 1973); for 2.5–5.0 m tall conifer saplings with wind speeds between 4 and 20 m s⁻¹ C_{Dv} varied between 1.5 and 0.2 (Rudnicki et al., 2004); and, for five hardwood species C_{Dv} varied between 1.02 and 0.10 (Vollsinger et al., 2005). Conclusions are similar in the field, where Koizumi et al. (2010) report C_{Dv} for three poplar tree crowns varying from 1.1 to 0.1 with wind speeds between 1 and 15 m s⁻¹. These results indicate at high wind speeds the relative drag of an individual tree ($C_{Dv} \sim 0.1$ –0.2) is small compared to that of buildings, but during some flow conditions C_{Dv} can approach that of a solid structure of similar shape (i.e. 1.2) and therefore exert similar drag to buildings.

The state of foliage on a tree (i.e. porosity) influences the amount of drag exerted on the flow. Koizumi et al.'s (2010) field observations at wind speeds of 10 m s⁻¹ found C_{Dv} to over halve when tree crowns are defoliated (i.e. more porous). Current understanding of C_{Dv} variability with porosity is based upon artificial (i.e. two-dimensional) and natural (i.e. tree or tree model) wind break studies. Hagen and Skidmore (1971) found C_{Dv} to be similar to single tree values: $C_{Dv} \sim 0.5$ for one row deciduous windbreaks and $C_{Dv} \sim 0.6$ –1.2 for coniferous windbreaks. Guan et al.'s (2003, their Table 5) synthesis of C_{Dv} for two-dimensional structures or naturally vegetated windbreaks of varying porosity provides a relation between C_{Dv} and porosity (P_{3D}):

$$C_{Dv} = 1.08(1 - P_{3D}^{1.8}) \quad (6)$$

Similarly, for an isolated model tree, Guan et al. (2000) show:

$$C_{Dv} = -1.251P_{3D}^2 + 0.489P_{3D} + 0.803 \quad (7)$$

Results of previous studies (summarised in Fig. 1) indicate that more impermeable roughness elements (i.e. $P_{3D} = 0$) tend to have the largest C_{Dv} , approaching that of a solid structure (0.8–1.2). As aerodynamic porosity increases, C_{Dv} decreases approximately as a power function to zero for an open surface (i.e. $P_{3D} = 1$). Observations by Grant and Nickling (1998) for a single conifer tree (Fig. 1, GN) and wind tunnel studies by Guan et al. (2000) support evidence that the relation may peak at critical porosities (Grant and Nickling, 1998; Gillies et al., 2002).

2.3. Parameter determination and method development

In the methodology proposed here, the H_{av} , H_{max} and σ_H of all roughness elements (i.e. buildings and vegetation) are determined.

Porosity is accounted for when determining λ_p as vegetation has openings in the volume it occupies. The plan area of vegetation (A_{pv}) is reduced by a porosity factor (i.e. $1 - P_{3D}$). The λ_p of both buildings and

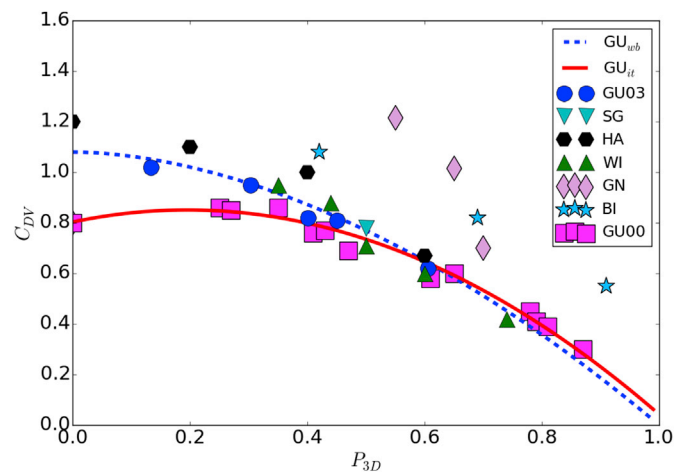


Fig. 1. Relation between the drag coefficient of porous roughness elements (C_{Dv}) and porosity (P_{3D}), data from: Hagen and Skidmore (1971) (HA); Wilson (1985) (WI); Seginer (1975) (SG); Grant and Nickling (1998) (GN); Bitog et al. (2011) (BI), Guan et al. (2000) (GU00) and Guan et al. (2003) (GU03). Lines are relations from Guan et al. (2003) (GU_{wb}, Eq. (6)) and Guan et al. (2000) (GU_{it}, Eq. (7)).

porous vegetation becomes:

$$\lambda_p = \frac{\sum_{i=1}^n A_{pbi} + \sum_{j=1}^n (1 - P_{3D}) A_{pvj}}{A_T} \quad (8)$$

where A_{pb} is the plan area of buildings and i or j refers to each individual built or vegetated roughness element, respectively.

The *Mac* method (Sect. 2.1) considers the drag balance at the top of a group of homogeneous roughness elements (of height z) approached by a logarithmic wind profile. If the roughness elements are of variable height, z is replaced by their average height (H_{av}) (Macdonald et al., 1998). Numerical models demonstrate the relative impact of trees and buildings represented by the drag coefficient are not affected by each other and neither is the spatially-averaged flow (Krayenhoff et al., 2015). Therefore, the total surface drag (F_D) can be determined as a combination of the drag from buildings (F_{Db}) and vegetation (F_{Dv}). Using the unsheltered frontal areas of buildings (A^{*fb}), the drag at the building tops (height H_{av}) can be written (e.g. Millward-Hopkins et al., 2011):

$$F_{Db} = 0.5\rho C_{Db} U_z^2 A^{*fb} \quad (9)$$

and similarly, for still-air impermeable vegetation (A^{*fv}) the drag on vegetation (F_{Dv}) is:

$$F_{Dv} = 0.5\rho C_{Dv} U_z^2 A^{*fv} \quad (10)$$

with ρ the density of air. The total drag of both the buildings and vegetation per unit area is therefore:

$$\tau = \frac{F_{Db} + F_{Dv}}{A_T} = \rho u_s^2 = \frac{0.5\rho C_{Db} U_z^2 A^{*fb} + 0.5\rho C_{Dv} U_z^2 A^{*fv}}{A_T} \quad (11)$$

As the *Mac* method assumes the drag below the zero-plane displacement is negligible, the unsheltered frontal area exerting drag on the flow consists of only roughness-element frontal area above z_d . Therefore, Mac_{z_d} is calculated (Eq. (2)) with the influence of vegetation incorporated through H_{av} and in the porosity parameterisation used in λ_p (Eq. (8)). Since all roughness elements are assumed homogeneous in height, the relation between the unsheltered frontal areas of buildings and vegetation (A^{*f}) and their actual frontal areas (A_f) is:

$$A_f = \frac{z}{z - z_d} A^{*f} \quad (12)$$

The unsheltered frontal areas (A^{*fb} and A^{*fv}) in Eq. (11) can be replaced

by actual frontal areas (A_{fb} and A_{fv}):

$$\frac{0.5\rho C_{Db} U_z^2 \left(1 - \frac{z_d}{z}\right) A_{fb} + 0.5\rho C_{Dv} U_z^2 \left(1 - \frac{z_d}{z}\right) A_{fv}}{A_T} = \rho u_*^2 \quad (13)$$

Common factors are removed from the numerator on the left-hand side of Eq. (13). To state Eq. (13) in terms of C_{Db} only, the ratio of C_{Dv} and C_{Db} is used (P_v). Using the variation of C_{Dv} with porosity for a single tree, the Guan et al. (2000) relation (Eq. (7)) gives:

$$P_v = \frac{C_{Dv}}{C_{Db}} = \frac{-1.251P_{3D}^2 + 0.489P_{3D} + 0.803}{C_{Db}} \quad (14)$$

Accounting for differential drag imposed by buildings and vegetation through P_v , Eq. (13) may then be written:

$$0.5\rho C_{Db} U_z^2 \left(1 - \frac{z_d}{z}\right) \frac{\{A_{fb} + (P_v)A_{fv}\}}{A_T} = \rho u_*^2 \quad (15)$$

When substituted into the logarithmic wind law (Eq. (1)), cancellation and inclusion of the drag correction coefficient (β) proposed by Macdonald et al. (1998) provides z_0 :

$$\frac{z_0}{z} = \left(1 - \frac{z_d}{z}\right) \exp \left[- \left(\frac{1}{\kappa^2} 0.5\beta C_{Db} \left(1 - \frac{z_d}{z}\right) \frac{\{A_{fb} + (P_v)A_{fv}\}}{A_T} \right)^{-0.5} \right] \quad (16)$$

Equation (16) is analogous to Macdonald et al.'s (1998) (Eq. (3)). However, the frontal area of buildings and vegetation are determined separately and P_v is included within the λ_f term to describe the differential drag of buildings and vegetation of varying porosity.

It should be noted that the calculated frontal area of vegetation A_{fv} is independent of porosity. A_{fv} is determined assuming a solid structure

with the same dimensions. Vegetation's influence upon z_0 is a consequence of the change in the drag coefficient for vegetation with porosity (P_v , Eq. (14)). Additionally, β is observed to be unity for staggered arrays of solid cubes. Without further experimentation upon arrays consisting of porous and solid roughness elements it is inappropriate to apply the drag correction to arrays including vegetation. Therefore, if any value other than unity is used for β , P_v should be further reduced:

$$P_v = \frac{-1.251P_{3D}^2 + 0.489P_{3D} + 0.803}{\beta C_{Db}} \quad (17)$$

2.4. Demonstration of impact

Behaviour of the parameterisation is demonstrated for five study areas selected from a surface elevation database for Greater London (Lindberg and Grimmond, 2011). Study areas are selected to characterise different urban spaces in a European city (roughness elements with heights > 2 m): city centre with low vegetation (Fig. 2a, CC_lv), city centre with similar building and vegetation height (Fig. 2b, CC_hv), suburban area with low vegetation (Fig. 2c, Sb_lv), suburban area with tall vegetation (Fig. 2d, Sb_hv) and an urban park (Fig. 2e, Pa).

Geometric and aerodynamic parameters for each study area are calculated iteratively (Kent et al., 2017a methodology) using the Kormann and Meixner (2001) analytical source area footprint model. For each study area, the same meteorological conditions observed by a CSAT3 sonic anemometer (Campbell Scientific, USA) in central London (King's College London, Strand Campus, height 50.3 m above ground level, see Kotthaus and Grimmond, 2012, 2014a, b for methods) are used. The median meteorological conditions of the fastest 25% of winds in 2014 (30-min averages) are used. Inputs to the footprint model are: measurement height (z) = 50.3 m; standard deviation of the lateral wind velocity (σ_v) = 1.97 m s⁻¹, Obukhov length (L) = - 1513 m;

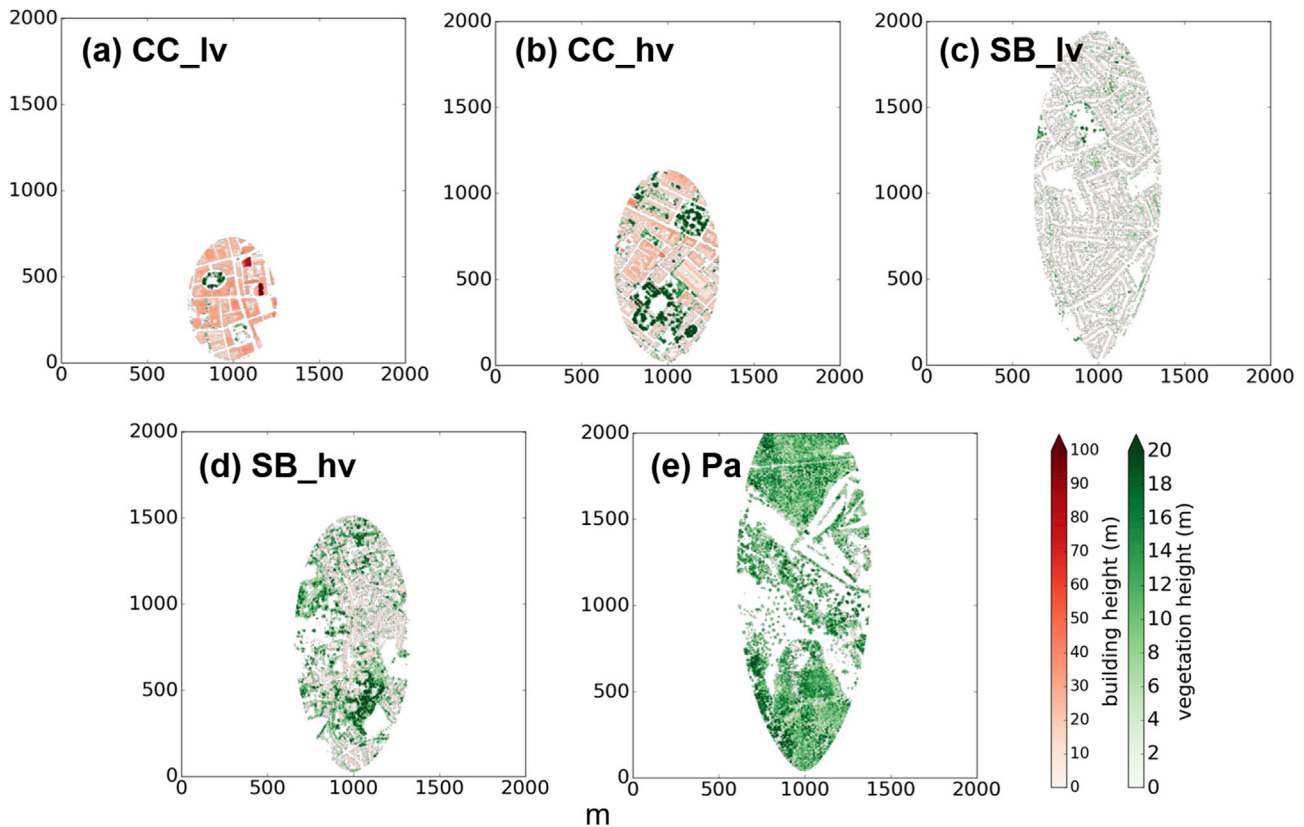


Fig. 2. Study areas representative of: (a) city centre with low vegetation (CC_lv), (b) city centre with similar building and vegetation heights (CC_hv), (c) suburban with low vegetation (Sb_lv), (d) suburban with taller vegetation (Sb_hv) and (e) an urban park (Pa). Source areas determined using the iterative methodology of Kent et al. (2017a), rotated into the wind direction (210°). Colour indicates roughness-element type and hue its height (see key). Axes labels are distance in metres.

Table 1

Geometric parameters determined for: all roughness elements; vegetation only; and buildings only, in the five study areas (Fig. 2). H_{av} , H_{max} and σ_H are the average, maximum and standard deviation of roughness-element heights (in metres), respectively, λ_p is plan area index and λ_f is frontal area index. Subscripts: v for vegetation, b for buildings, $l-on$ for leaf-on and $l-off$ for leaf-off.

Area	All							Vegetation					Buildings					
	H_{av}	H_{max}	σ_H	$\lambda_{p,l-on}$	$\lambda_{p,l-off}$	$\lambda_{f,l-on}^a$	$\lambda_{f,l-off}^a$	$H_{av,v}$	$H_{max,v}$	$\sigma_{H,v}$	$\lambda_{p,v,l-on}$	$\lambda_{p,v,l-off}$	$\lambda_{f,v}$	$H_{av,b}$	$H_{max,b}$	$\sigma_{H,b}$	$\lambda_{p,b}$	$\lambda_{f,b}$
CC_lv	23.50	125.00	15.00	0.54	0.52	0.52	0.51	10.90	35.00	8.78	0.03	0.01	0.04	24.50	125.00	15.00	0.51	0.49
CC_hv	14.90	46.60	7.99	0.48	0.37	0.42	0.37	15.70	34.00	7.47	0.21	0.11	0.26	14.10	46.60	8.22	0.27	0.23
SB_lv	5.34	27.80	2.64	0.29	0.25	0.18	0.17	4.82	27.80	3.46	0.08	0.04	0.08	5.58	16.60	2.00	0.21	0.13
SB_hv	10.80	33.30	5.37	0.47	0.33	0.33	0.28	11.60	33.30	5.78	0.29	0.14	0.29	9.12	28.10	3.75	0.18	0.12
Pa	11.30	29.00	4.67	0.60	0.30	0.29	0.22	11.40	29.00	4.63	0.59	0.30	0.41	5.75	16.50	2.39	0.00	0.00

^a $\lambda_{f,l-on}$ and $\lambda_{f,l-off} = \left[\frac{\lambda_b + (P_v)\lambda_b}{A_T} \right]$, assuming a leaf-on and leaf-off porosity, respectively.

$u_* = 0.94 \text{ m s}^{-1}$; wind direction 210° ; z_d and z_0 . Source area calculations are initiated with open country values for the aerodynamic parameters ($z_d = 0.2 \text{ m}$, $z_0 = 0.03 \text{ m}$), as the final values are insensitive to this initial assumption (Kent et al., 2017a). The source area analysed here is the cumulative total of 80% of the total source area.

Dynamic response of the source areas during the iterative procedure modifies the surface area considered. The initial source area is overlain upon the surface elevation databases (buildings and vegetation) for each study area and a weighted geometry is calculated, based upon the fractional contribution of each grid square in the source area. Source area specific aerodynamic parameters are determined, which are the input to the next iteration (the meteorological conditions and measurement height remain constant). Both buildings and vegetation are considered, assuming a leaf-on porosity of $P_{3D} = 0.2$, and leaf-off porosity of $P_{3D} = 0.6$ (more porous) (Heisler, 1984; Heisler and Dewalle, 1988; Grimmond and Oke, 1999).

Variations in meteorological conditions between sites probably occur, however the objective to obtain representative study areas (Fig. 2a–e, Table 1) means the assumption of constant conditions is treated as reasonable. The resulting geometry and (*Mac* and *Kan*) aerodynamic parameters are compared for each study area (Sect. 3.1 and 3.2).

Using the logarithmic wind law (Eq. (1)) the implications of considering vegetation during wind-speed estimation close to the surface are then assessed (Sect. 3.3). Using the z_d and z_0 determined for buildings only, or both buildings and vegetation, for the five study areas, wind speeds are extrapolated from $z_d + z_0$ to 100 m using Eq. (1). For consistency, at $z_d + z_0$ it is assumed the wind speed is 0 m s^{-1} and throughout the profile the previously stated central London friction velocity ($u_* = 0.94 \text{ m s}^{-1}$) is assumed. Although choosing a different value of u_* will have implications for the estimated wind speeds, the relative magnitude of change for each profile is the same and therefore so are the percentage differences between profiles. The objective is to demonstrate the implications of considering (or not) vegetation for each morphometric method and study area, as opposed to providing a comparison between the study areas.

Table 2

Aerodynamic parameters determined using the Macdonald et al. (1998, *Mac*) and Kanda et al. (2013, *Kan*) morphometric methods in the five study areas (Fig. 2). Parameters are determined for buildings only and for all roughness elements (both buildings and vegetation), with leaf-on (*l-on*) and leaf-off (*l-off*) vegetation.

Area	<i>Mac</i>						<i>Kan</i>					
	z_0		z_d				z_0		z_d			
	Buildings	All		Buildings	All		Buildings	All		Buildings	All	
<i>l-on</i>		<i>l-off</i>	<i>l-on</i>		<i>l-off</i>	<i>l-on</i>		<i>l-off</i>	<i>l-on</i>		<i>l-off</i>	
CC_lv	1.21	1.01	1.10	18.84	18.67	18.41	2.96	2.86	2.98	44.53	44.34	43.94
CC_hv	1.48	0.78	1.30	7.19	11.11	9.57	1.62	1.44	1.78	19.92	24.65	22.72
SB_lv	0.48	0.41	0.48	2.36	2.88	2.58	0.37	0.42	0.44	6.29	7.56	7.22
SB_hv	0.89	0.49	0.98	3.42	7.91	6.28	0.68	0.80	1.10	10.16	17.25	15.29
Pa	0.00	0.18	0.99	0.05	9.44	6.24	0.00	0.32	0.92	2.07	18.33	14.58

Buildings	
All	leaf-on
	leaf-off

Table 3

Percentage difference in aerodynamic parameters calculated using the (a) *Macdonald et al. (1998)* and (b) *Kanda et al. (2013)* morphometric methods from Table 2, between: buildings (x) and all roughness elements (y) assuming a leaf-on porosity (b, *l-on*); buildings (x) and all roughness elements (y) assuming a leaf-off porosity (b, *l-off*) and for all roughness elements assuming a leaf-on (x) or leaf-off porosity (y) (*l-on*, *l-off*). Percentage difference = $\frac{|x-y|}{(x+y)/2} \times 100$.

(a) <i>Mac</i>	z_0			z_d		
	<i>b, l-on</i>	<i>b, l-off</i>	<i>l-on, l-off</i>	<i>b, l-on</i>	<i>b, l-off</i>	<i>l-on, l-off</i>
CC_lv	18.37	9.88	8.53	0.86	2.31	1.45
CC_hv	62.48	13.53	50.00	42.75	28.30	14.91
SB_lv	15.47	0.51	14.96	19.72	8.90	10.87
SB_hv	57.25	10.01	66.31	79.37	59.08	22.98
Pa	-	-	137.58	197.90	196.83	40.73
(b) <i>Kan</i>	z_0			z_d		
	<i>b, l-on</i>	<i>b, l-off</i>	<i>l-on, l-off</i>	<i>b, l-on</i>	<i>b, l-off</i>	<i>l-on, l-off</i>
CC_lv	3.68	0.44	4.12	0.42	1.32	0.90
CC_hv	11.67	9.47	21.08	21.22	13.12	8.16
SB_lv	12.57	18.10	5.56	18.37	13.78	4.62
SB_hv	16.70	46.76	30.66	51.74	40.36	12.01
Pa	-	-	96.76	159.38	150.23	22.80

% difference
< 10
10 < % < 25
25 < % < 50
50 < % < 100
> 100

Table 4

Percentage difference in aerodynamic parameters calculated using the *Macdonald et al. (1998, Mac)* (x) or *Kanda et al. (2013, Kan)* (y) morphometric methods from Table 2, for buildings only and all roughness elements assuming a leaf-on porosity (*l-on*) and leaf-off porosity (*l-off*). Percentage difference = $\frac{|x-y|}{(x+y)/2} \times 100$.

Area	Buildings		All			
	z_0	z_d	<i>l-on</i>		<i>l-off</i>	
			z_0	z_d	z_0	z_d
CC_lv	83.69	81.09	95.47	81.46	92.03	81.91
CC_hv	8.44	93.88	59.54	75.76	31.22	81.49
SB_lv	26.33	90.68	1.61	89.60	7.81	94.53
SB_hv	26.65	99.31	47.88	74.19	10.81	83.52
Pa	34.07	190.60	53.76	64.09	8.10	80.10

% difference
< 10
10 < % < 25
25 < % < 50
50 < % < 100
> 100

3.2. Aerodynamic parameters

For aerodynamic parameter determination, the geometric parameters

within the morphometric methods (e.g. *Kan* considers height variability) are important, in addition to the dominance of either buildings or vegetation. For a heterogeneous group of roughness elements *Kan_{z_d}* is

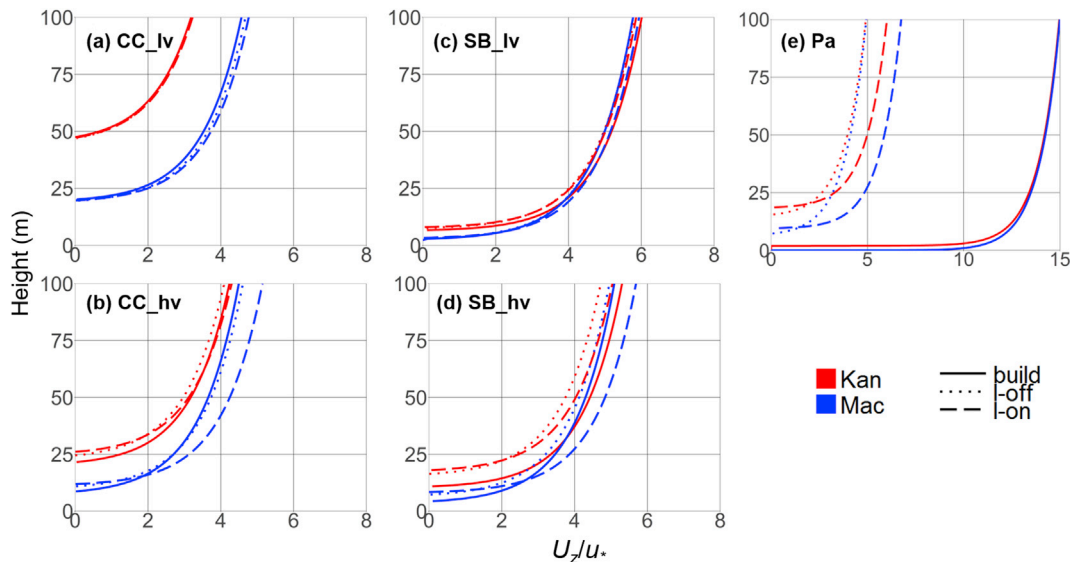


Fig. 3. Logarithmic wind-speed profiles (using Eq. (1)) from $z = z_d + z_0$ to $z = 100$ m, using z_d and z_0 determined for five study areas: (a) city centre with low vegetation (CC_lv), (b) city centre with similar building and vegetation heights (CC_hv), (c) a suburb with low vegetation (SB_lv), (d) a suburb with taller vegetation (SB_hv) and (e) a park (Pa). Wind speed at the bottom of the profile ($z_d + z_0$) is assumed 0 m s^{-1} and friction velocity (u_*) 0.94 m s^{-1} throughout the profile. Wind speeds are normalised by u_* (U_z/u_*). Aerodynamic parameters are determined using the *Kanda et al. (2013)* (*Kan*) and *Macdonald et al. (1998)* (*Mac*) morphometric methods for each study area, considering buildings only (solid line), including vegetation with leaf-off porosity (short dashed line) and leaf-on porosity (long dashed line) (values in Table 2). Note different x scale on (e).

typically twice as large as Mac_{z_d} at all densities. Mac_{z_0} is observed to be larger than Kan_{z_0} at λ_f below ~ 0.25 , beyond which Kan_{z_0} is larger (Kent et al., 2017a; their Fig. 1).

Generally, accounting for vegetation (with buildings) increases z_d because the increase in plan area acts to 'close' the canopy and therefore lift the zero-plane displacement (Table 2). The effect is most obvious during leaf-on and where there is a higher density of vegetation (SB_hv, Pa). This creates a greater than 40% difference between z_d calculated for buildings alone and the combined case (buildings and vegetation). CC_lv is the only area where considering vegetation may reduce z_d because a small increase in λ_p is offset by a reduction in H_{av} (Table 2). Leaf-on z_d is always greater than leaf-off, but the difference is less obvious for the Kan method as height variability (in addition to λ_p) is accounted for.

Kan_{z_d} is consistently the order of H_{av} (or larger) and typically over double Mac_{z_d} (Table 2). The range of percentage change for z_d caused by vegetation inclusion and its state (Table 3) tend to be over half the inter-method variability of Kan_{z_d} and Mac_{z_d} (Table 4). Thus, the priority of decisions for accurate determination of z_d is firstly selection of the appropriate morphometric method, followed by the inclusion of vegetation and then its state (leaf-on or leaf-off). An exception is in Pa, where vegetation has the largest effect.

The effect of considering vegetation for z_0 depends upon: the height based geometric parameters, the increase in λ_f and λ_p ; and the associated change in z_d . The inter- and intra-method differences of Mac and Kan depend upon their response to changes in λ_f . Both methods indicate z_0 increases from zero to a maximum value at a critical λ_f (λ_{f-crit}), after which z_0 decreases again. For Mac_{z_0} , λ_{f-crit} is between ~ 0.15 – 0.25 and for Kan_{z_0} this is 0.2 – 0.4 (Kent et al., 2017a; their Fig. 1). At larger λ_f , there is a steeper decline in Mac_{z_0} than Kan_{z_0} .

When an already large built frontal area is further increased due to the vegetation (CC_lv, CC_hv), leaf-on z_0 becomes smaller for both methods as there is a shift further away from λ_{f-crit} . For both CC_lv and CC_hv the percentage changes are larger for Mac_{z_0} than Kan_{z_0} given the sensitivity of the former to changes of λ_f . The reduction is greater for leaf-on because of the larger λ_f (Table 1).

In locations with low built frontal areas (Table 1, SB_hv, SB_lv) the inclusion of vegetation should increase Mac_{z_0} and Kan_{z_0} given they move towards λ_{f-crit} . This is true for Kan_{z_0} , most obviously in SB_hv (17% difference for leaf-on and 47% for leaf-off, Table 3) where vegetation is more dominant and H_{max} , σ_H and λ_p become obviously larger. However, for Mac_{z_0} , the λ_f increase is offset by the concurrent increase in z_d (Table 2). Therefore Mac_{z_0} decreases for leaf-on conditions, but is similar for leaf-off. For Pa, inclusion of vegetation means $Mac_{z_0,b}$ and $Kan_{z_0,b}$ both increase from 0 m to 0.18 and 0.32 m, respectively during leaf-on, and to 0.99 and 0.92 m, respectively for leaf-off (Table 2). If only buildings are considered, the variability between $Kan_{z_0,b}$ and $Mac_{z_0,b}$ is less than 35% in all study areas apart from CC_lv, where $Kan_{z_0,b}$ is more than double $Mac_{z_0,b}$ because of the large $\lambda_{f,b}$ (~ 0.5).

Leaf-on z_0 is consistently smaller than leaf-off for both morphometric methods as a consequence of both λ_f and z_d increasing. The greater sensitivity of Mac_{z_0} to λ_f results in a percent difference that is twice that of Kan_{z_0} , except in Pa where both experience large increases (Table 3). During leaf-off, areas with λ_f similar to λ_{f-crit} (e.g. SB_lv, SB_hv) have mean inter-method variability of $\sim 10\%$. Whereas if there are already high λ_f (SB_hv, CC_hv and CC_lv), an increase in λ_f with leaf-on vegetation causes inter-method variability to increase, ranging between 48 and 95% (Table 4).

Therefore, if buildings dominate (e.g. CC_hv) selection of the appropriate morphometric method is more critical for determining z_0 (causing a larger percentage difference in z_0) than if vegetation is included. The inclusion of vegetation increases inter-method variability between the two morphometric methods (e.g. CC_hv and CC_lv). Where there is more vegetation, its inclusion and state (leaf-on or off), is as or more important than the inter-method variability in z_0 . This is especially true for Pa.

3.3. Influence of considering vegetation upon wind

Accurately modelling the spatially- and temporally-averaged wind-speed profile above urban surfaces is critical for numerous applications, including dispersion studies and wind load determination. Various methods to estimate the wind-speed profile exist, each developed from different conditions and with different inherent assumptions (e.g. Deaves and Harris, 1978; Emeis et al., 2007; Gryning et al., 2007). However, the aerodynamic roughness parameters (z_d and z_0) are consistently used to represent the underlying surface. Although only two methods to determine the roughness parameters are used here (Mac and Kan), a range of methods exist which can influence wind-speed estimations (Kent et al., 2017a).

Using the logarithmic wind law (Eq. (1)), wind-speeds extrapolated using the Kan method tend to be less than those using Mac (Fig. 3a–e) because of the considerably larger Kan_{z_0} . Notably, where z_d is largest in magnitude (e.g. CC_lv, Table 2) wind speeds at 100 m calculated using the Kan or Mac aerodynamic parameters vary between 36 and 39% of each other (depending on vegetation state). Elsewhere, extrapolated wind speeds tend to be more similar, and the least variable aerodynamic parameters in SB_lv and SB_hv mean wind speeds at 100 m vary by less than 4% and 12%, respectively.

The difference in wind speed when both buildings and vegetation are accounted for (Fig. 3, dashed lines), in comparison to buildings alone (Fig. 3, solid lines) is least where buildings dominate. For example, in CC_lv and SB_lv vegetation has little effect and regardless of its state causes a maximum wind-speed variation of $<5\%$ for each respective morphometric method.

Consideration of vegetation in the morphometric methods has a greater influence upon predicted wind speeds where vegetation is taller and more abundant (e.g. CC_hv, SB_hv and Pa). In addition, vegetation state (i.e. leaf-on or leaf-off) is more influential upon wind speeds in these areas. Despite z_d increasing with inclusion of vegetation, there is greater inter- and intra-method variability in z_0 (Sect. 3.2). Therefore, because estimated wind profiles are a function of both z_d and z_0 no general comment can be made about wind-speed changes when including vegetation.

Vegetation's effect is most noticeable in Pa. High wind speeds when only buildings are considered (because of low z_d and z_0) are reduced by almost a factor of three upon consideration of vegetation (Fig. 3e). The reduction in wind speed is more obvious for leaf-off porosities, because of the larger associated z_0 . In CC_hv and SB_hv the effect of vegetation is less obvious, however a decrease in z_0 means wind speeds extrapolated using the Mac parameters increase. In contrast, wind speeds extrapolated using the Kan parameters tend to decrease because of the larger z_d and lesser sensitivity to changes in z_0 (Sect. 3.2).

In summary, when buildings dominate (CC_lv) the morphometric method chosen to determine the wind profile (i.e. Mac or Kan) is more important than whether vegetation is considered. In contrast, where vegetation is taller and accounts for a greater surface area (CC_hv, SB_hv and especially Pa) vegetation's consideration has larger implications for wind-speed estimation than the morphometric method used. In all cases, the differences between leaf-on and leaf-off wind speed are larger for the Mac than Kan method, because of the sensitivity of Mac to the porosity parameterisation.

4. Conclusions

Vegetation should be included in morphometric determination of aerodynamic parameters, but not in the same way as solid structures. A methodology is proposed to include vegetation in Macdonald et al.'s (1998) morphometric method to determine the zero-plane displacement (z_d) and aerodynamic roughness length (z_0). This also applies to Kanda et al.'s (2013) extension, which considers roughness-element height variability.

The proposed methodology considers the average, maximum and

standard deviation of heights for all roughness elements (buildings and vegetation). The plan area index and frontal area index of buildings and vegetation are determined separately (and subsequently combined for use in the morphometric methods). Aerodynamic porosity is used to determine the plan area of vegetation. Whereas, the frontal area index of vegetation is determined assuming a solid structure with the same dimensions. During determination of z_0 a parameterisation of the drag coefficient for vegetation is used, accounting for varying porosity. This follows literature that demonstrates the drag exerted by trees can be like that of a solid structure and decreases as porosity increases (Grant and Nickling, 1998; Guan et al., 2000; Vollsinger et al., 2005; Koizumi et al., 2010). The relation between the drag coefficient and porosity of an individual tree (Guan et al., 2000) is used as the basis for the parameterisation, which other experimental data demonstrate is reasonable.

From analysis of five different urban areas within a European city, the effect of the inclusion of vegetation on geometric and aerodynamic parameters depends upon whether buildings or vegetation are the dominant roughness element. Where buildings are taller they control the height-based geometric parameters. The opposite is true when vegetation is taller. Inclusion of vegetation increases the plan area index (λ_p) and frontal area index (λ_f), most obviously during leaf-on periods.

The increases in λ_p and λ_f from inclusion of vegetation more obviously affect aerodynamic parameters than the change in height based geometric parameters. The higher λ_p produces a larger z_d for both morphometric methods in four study areas. In the fifth case, a reduction in average height offsets the increase in λ_p . The increase in z_d is largest for leaf-on because of the higher λ_p , as well as where vegetation is taller and more significant because of the greater increase in λ_p and average height (H_{av}). Given the large inter-method variability in z_d , selection of the appropriate morphometric method is most critical, followed by whether vegetation is considered, then by the vegetation state (leaf-on or leaf-off).

Inclusion of the effect of vegetation on z_0 depends upon: the geometric parameters determined without vegetation and the associated λ_f that the peak z_0 occurs for each morphometric method. Therefore, a broad statement about how z_0 responds to vegetation inclusion is difficult. However, the change in z_0 is more obvious where vegetation is taller and takes up a large proportion of area. In the same areas, whether vegetation is included and its state (i.e. porosity) is as, or more important, than the inter-method variability in z_0 determined by the morphometric methods. Leaf-on z_0 is consistently smaller than leaf-off, because of the combined increase in λ_f and z_d which create an effectively smoother surface.

Assuming a logarithmic wind profile, the influence on estimated wind speed up to 100 m is least when vegetation is lower and accounts for a smaller proportion of surface area, with wind speed varying by < 5% regardless of consideration of vegetation. In contrast, wind speeds above an urban park are demonstrated to be slowed by up to a factor of three (both methods). Therefore, if vegetation is taller and more abundant, vegetation's inclusion is as, or more, critical for wind-speed estimation than the morphometric method used.

Of course, the ultimate assessment of the parameterisation for accurate aerodynamic parameter and wind-speed estimation is comparison to observations. An assessment of the parameterisation, demonstrates the seasonal change in aerodynamic parameters can be captured and wind-speed estimations improved (Kent et al. 2017b). Undoubtedly, further observations and wind tunnel experiments with various arrays of solid and porous roughness elements will be valuable to assess the parameterisation.

Funding

This work is funded by a NERC CASE studentship in partnership with Risk Management Solutions (NE/L00853X/1) and the Newton Fund/Met Office CSSP China. Observations used in these analyses are funded from NERC ClearFlo (KCL and Reading), EU7 BRIDGE, EU7 emBRACE, H2020 UrbanFluxes, EPSRC BTG, KCL and University of Reading.

Acknowledgements

The numerous people who maintain the daily operations, collection and processing of data for the London Urban Meteorological Observatory (LUMO) network (<http://micromet.reading.ac.uk/>), including Will Morrison and Kjell zum Berge. King's College London support for provision of the sites. The morphometric method development (including vegetation) and source area calculation are implemented into the Urban Multi-scale Environmental Predictor (UMEP, <http://www.urban-climate.net/umep/UMEP>) climate service plugin for the open source software QGIS.

References

- Amiro, B., 1990. Drag coefficients and turbulence spectra within three boreal forest canopies. *Boundary-Layer Meteorol.* 52, 227–246.
- Bitog, J., Lee, I., Hwang, H., Shin, M., Hong, S., Seo, I., Mostafa, E., Pang, Z., 2011. A wind tunnel study on aerodynamic porosity and windbreak drag. *For. Sci. Technol.* 7, 8–16.
- Cheng, H., Hayden, P., Robins, A.G., Castro, I.P., 2007. Flow over cube arrays of different packing densities. *J. Wind Eng. Ind. Aerodyn.* 95, 715–740.
- Crow, P., Benham, S., Devereux, B., Amable, G., 2007. Woodland vegetation and its implications for archaeological survey using LiDAR. *Forestry* 80, 241–252.
- da Costa, J.L., Castro, F., Palma, J., Stuart, P., 2006. Computer simulation of atmospheric flows over real forests for wind energy resource evaluation. *J. Wind Eng. Ind. Aerodyn.* 94, 603–620.
- Deaves, D., Harris, R., 1978. A Mathematical Model of the Structure of Strong Winds. Report number 76. Construction Industry Research and Information Association, London, England.
- Drew, D.R., Barlow, J.F., Lane, S.E., 2013. Observations of wind speed profiles over Greater London, UK, using a Doppler lidar. *J. Wind Eng. Ind. Aerodyn.* 121, 98–105.
- Emeis, S., Baumann-Stanzer, K., Piringer, M., Kallistratova, M., Kouznetsov, R., Yushkov, V., 2007. Wind and turbulence in the urban boundary layer—analysis from acoustic remote sensing data and fit to analytical relations. *Meteorol. Z.* 16, 393–406.
- Finnigan, J., 2000. Turbulence in plant canopies. *Annu. Rev. Fluid Mech.* 32, 519–571.
- Gillies, J., Lancaster, N., Nickling, W., Crawley, D., 2000. Field determination of drag forces and shear stress partitioning effects for a desert shrub (*Sarcobatus vermiculatus*, greasewood). *J. Geophys. Res. D. Atmos.* 105, 24871–24880.
- Gillies, J., Nickling, W., King, J., 2002. Drag coefficient and plant form response to wind speed in three plant species: burning Bush (*Euonymus alatus*), Colorado Blue Spruce (*Picea pungens glauca.*), and Fountain Grass (*Pennisetum setaceum*). *J. Geophys. Res. D. Atmos.* 107, 4760.
- Grant, P., Nickling, W., 1998. Direct field measurement of wind drag on vegetation for application to windbreak design and modelling. *Land Degrad. Dev.* 9, 57–66.
- Grimmond, C.S.B., Oke, T.R., 1999. Aerodynamic properties of urban areas derived from analysis of surface form. *J. Appl. Meteorol. Clim.* 38, 1262–1292.
- Gromke, C., Ruck, B., 2009. On the impact of trees on dispersion processes of traffic emissions in street canyons. *Boundary-Layer Meteorol.* 131, 19–34.
- Gryning, S., Batchvarova, E., Brümmner, B., Jørgensen, H., Larsen, S., 2007. On the extension of the wind profile over homogeneous terrain beyond the surface boundary layer. *Boundary-Layer Meteorol.* 124, 251–268.
- Guan, D., Ting-Yao, Z., Shi-Jie, H., 2000. Wind tunnel experiment of drag of isolated tree models in surface boundary layer. *J. For. Res.* 11, 156–160.
- Guan, D., Zhang, Y., Zhu, T., 2003. A wind-tunnel study of windbreak drag. *Agric For Meteorol.* 118, 75–84.
- Guan, W., Li, C., Li, S., Fan, Z., Xie, C., 2002. Improvement and application of digitized measure on shelterbelt porosity. *J. Appl. Ecol.* 13, 651–657.
- Hagen, L., Skidmore, E., 1971. Windbreak drag as influenced by porosity. *Trans. ASAE* 14, 464–465.
- Hall, D., Macdonald, J.R., Walker, S., Spanton, A.M., 1996. Measurements of Dispersion within Simulated Urban Arrays—a Small Scale Wind Tunnel Study. BRE Client Report, CR178/96.
- Heisler, G.M., 1984. Measurements of solar radiation in the shade of individual trees. In: Hutchinson, B.A., Hicks, B.B. (Eds.), *The Forest-Atmosphere Interaction*. Springer, Netherlands, pp. 319–355.
- Heisler, G.M., Dewalle, D.R., 1988. Effects of windbreak structure on wind flow. *Agric. Ecosyst. Environ.* 22, 41–69.
- Högström, U., 1996. Review of some basic characteristics of the atmospheric surface layer. *Boundary-Layer Meteorol.* 28, 215–246.
- Holland, D.E., Berglund, J.A., Spruce, J.P., McKellip, R.D., 2008. Derivation of effective aerodynamic surface roughness in urban areas from airborne lidar terrain data. *J. Appl. Meteorol. Clim.* 47, 2614–2626.
- Jacobs, A.F., 1985. The normal-force coefficient of a thin closed fence. *Boundary-Layer Meteorol.* 32, 329–335.
- Judd, M., Raupach, M., Finnigan, J., 1996. A wind tunnel study of turbulent flow around single and multiple windbreaks, part I: velocity fields. *Boundary-Layer Meteorol.* 80, 127–165.
- Kanda, M., Inagaki, A., Miyamoto, T., Gryschka, M., Raasch, S., 2013. A new aerodynamic parameterization for real urban surfaces. *Boundary-Layer Meteorol.* 148, 357–377.
- Katul, G.G., Mahrt, L., Poggi, D., Sanz, C., 2004. One-and two-equation models for canopy turbulence. *Boundary-Layer Meteorol.* 113, 81–109.

- Kent, C.W., Grimmond, C.S.B., Gatey, D., Barlow, J., Kotthaus, S., Lindberg, F., Halios, C.H., 2017. Evaluation of urban local-scale aerodynamic parameters: implications for the vertical profile of wind speed and for source areas. *Boundary-Layer Meteorol.* <http://dx.doi.org/10.1007/s10546-017-0248-z>.
- Kent, C.W., Lee, K., Ward, H.C., Hong, J.W., Hong, J., Grimmond, C.S.B., 2017. Aerodynamic roughness variation with vegetation: analysis in a suburban neighbourhood and a city park (in review).
- Koizumi, A., Motoyama, J., Sawata, K., Sasaki, Y., Hirai, T., 2010. Evaluation of drag coefficients of poplar-tree crowns by a field test method. *J. Wood Sci.* 56, 189–193.
- Kormann, R., Meixner, F.X., 2001. An analytical footprint model for non-neutral stratification. *Boundary-Layer Meteorol.* 99, 207–224.
- Kotthaus, S., Grimmond, C.S.B., 2012. Identification of micro-scale anthropogenic CO₂, heat and moisture sources—processing eddy covariance fluxes for a dense urban environment. *Atmos. Environ.* 57, 301–316.
- Kotthaus, S., Grimmond, C.S.B., 2014a. Energy exchange in a dense urban environment—Part I: temporal variability of long-term observations in central London. *Urban Clim.* 10, 261–280.
- Kotthaus, S., Grimmond, C.S.B., 2014b. Energy exchange in a dense urban environment—Part II: impact of spatial heterogeneity of the surface. *Urban Clim.* 10, 281–307.
- Krayenhoff, E., Santiago, J., Martilli, A., Christen, A., Oke, T., 2015. Parametrization of drag and turbulence for urban neighbourhoods with trees. *Boundary-Layer Meteorol.* 156, 157–189.
- Lindberg, F., Grimmond, C.S.B., 2011. Nature of vegetation and building morphology characteristics across a city: influence on shadow patterns and mean radiant temperatures in London. *Urban Ecosyst.* 14, 617–634.
- Macdonald, R., Griffiths, R., Hall, D., 1998. An improved method for the estimation of surface roughness of obstacle arrays. *Atmos. Environ.* 32, 1857–1864.
- Mayhead, G., 1973. Some drag coefficients for British forest trees derived from wind tunnel studies. *Agric. Meteorol.* 12, 123–130.
- Millward-Hopkins, J., Tomlin, A., Ma, L., Ingham, D., Pourkashanian, M., 2011. Estimating aerodynamic parameters of urban-like surfaces with heterogeneous building heights. *Boundary-Layer Meteorol.* 141, 443–465.
- Mohammad, A., Zaki, S., Hagishima, A., Ali, M., 2015. Determination of aerodynamic parameters of urban surfaces: methods and results revisited. *Theor. Appl. Climatol.* 3, 635–649.
- Nakai, T., Sumida, A., Daikoku, K.I., Matsumoto, K., van der Molen, M.K., Kodama, Y., Kononov, A.V., Maximov, T.C., Dolman, A.J., Yabuki, H., Hara, T., 2008. Parametrisation of aerodynamic roughness over boreal, cool-and warm-temperate forests. *Agric. For. Meteorology* 148, 1916–1925.
- Pan, Y., Follett, E., Chamecki, M., Nepf, H., 2014. Strong and weak, unsteady reconfiguration and its impact on turbulence structure within plant canopies. *Phys. Fluids* 26, 105102.
- Rudnicki, M., Mitchell, S.J., Novak, M.D., 2004. Wind tunnel measurements of crown streamlining and drag relationships for three conifer species. *Can. J. For. Res.* 34, 666–676.
- Seginer, I., 1975. Atmospheric-stability effect on windbreak shelter and drag. *Boundary-Layer Meteorol.* 8, 383–400.
- Shaw, R.H., Patton, E.G., 2003. Canopy element influences on resolved-and subgrid-scale energy within a large-eddy simulation. *Agric For Meteorol* 115, 5–17.
- Shaw, R.H., Schumann, U., 1992. Large-eddy simulation of turbulent flow above and within a forest. *Boundary-Layer Meteorol.* 61, 47–64.
- Simiu, E., Scanlan, R.H., 1996. *Wind Effects on Structures*. Wiley, New York, p. 605.
- Su, H., Shaw, R.H., Paw, K.T., Moeng, C., Sullivan, P.P., 1998. Turbulent statistics of neutrally stratified flow within and above a sparse forest from large-eddy simulation and field observations. *Boundary-Layer Meteorol.* 88, 363–397.
- Suter-Burri, K., Gromke, C., Leonard, K.C., Graf, F., 2013. Spatial patterns of aeolian sediment deposition in vegetation canopies: observations from wind tunnel experiments using colored sand. *Aeolian Res.* 8, 65–73.
- Sutton, S., McKenna Neuman, C., 2008. Sediment entrainment to the lee of roughness elements: effects of vortical structures. *J. Geophys. Res. Earth Surf.* 113, F02S09.
- Taylor, P.A., 1988. Turbulent wakes in the atmospheric boundary layer. In: Steffen, W.L., Denmead, O.T. (Eds.), *Flow and Transport in the Natural Environment: Advances and Applications*. Springer, Berlin, pp. 270–292.
- Tennekes, H., 1973. The logarithmic wind profile. *J. Atmos. Sci.* 30, 234–238.
- Tieleman, H.W., 2008. Strong wind observations in the atmospheric surface layer. *J. Wind Eng. Ind. Aerodyn.* 96, 41–77.
- Van Renterghem, T., Botteldooren, D., 2008. Numerical evaluation of sound propagating over green roofs. *J. Sound. Vibrat* 317, 781–799.
- Vollsinger, S., Mitchell, S.J., Byrne, K.E., Novak, M.D., Rudnicki, M., 2005. Wind tunnel measurements of crown streamlining and drag relationships for several hardwood species. *Can. J. For. Res.* 35, 1238–1249.
- Vos, P.E., Maiheu, B., Vankerkom, J., Janssen, S., 2013. Improving local air quality in cities: to tree or not to tree? *Environ. Pollut.* 183, 113–122.
- Wilson, J.D., 1985. Numerical studies of flow through a windbreak. *J. Wind Eng. Ind. Aerodyn.* 21, 119–154.
- Wolfe, S.A., Nickling, W.G., 1993. The protective role of sparse vegetation in wind erosion. *Prog. Phys. Geogr.* 17, 50–50.
- Wyatt, V., Nickling, W., 1997. Drag and shear stress partitioning in sparse desert creosote communities. *Can. J. Earth Sci.* 34, 1486–1498.
- Yang, X., Yu, Y., Fan, W.A., 2017. A method to estimate the structural parameters of windbreaks using remote sensing. *Agrofor. Syst.* 91, 37–49.
- Zeng, P., Takahashi, H., 2000. A first-order closure model for the wind flow within and above vegetation canopies. *Agric For Meteorol* 103, 301–313.